On: 14 November 2013, At: 09:29
Publisher: Taylor & Francis
Informa Ltd Registered in England and Wales Registered Number: 1072954 Registered office: Mortimer House, 37-41 Mortimer Street, London W1T 3JH, UK

Separation Science and Technology
Publication details, including instructions for authors and subscription information:
http://www.tandfonline.com/loi/lsst20

Improvement in the Adsorption of Anionic and Cationic Dyes From Aqueous Solutions: A Comparative Study Using Aluminium Pillared Clays and Activated Carbon

J. E. Aguiar [a] , B. T. C. Bezerra [a] , A. C. A. Siqueira [a] , D. Barrera [b] , K. Sapag [b] , D. C. S. Azevedo [a] , S. M. P. Lucena [a] & I. J. Silva Jr. [a]

[a] Departamento de Engenharia Química , Universidade Federal do Ceará, Centro de Tecnologia, Grupo de Pesquisa em Separações por Adsorção - GPSA. Campus do Pici, Bloco 709 , CEP. 60455-760 , Fortaleza - CE , Brasil Phone: +55 (85) 3366-9611 (ext. 28) Fax: +55 (85) 3366-9611 (ext. 28)

[b] Laboratorio de Sólidos Porosos, INFAP-CONICET , Universidad Nacional de San Luis , San Luis , Argentina

Accepted author version posted online: 14 Nov 2013.Published online: 14 Nov 2013.

To cite this article: Separation Science and Technology (2013): Improvement in the Adsorption of Anionic and Cationic Dyes From Aqueous Solutions: A Comparative Study Using Aluminium Pillared Clays and Activated Carbon, Separation Science and Technology, DOI: 10.1080/01496395.2013.862720

To link to this article: http://dx.doi.org/10.1080/01496395.2013.862720

IMPROVEMENT IN THE ADSORPTION OF ANIONIC AND CATIONIC DYES FROM AQUEOUS SOLUTIONS: A COMPARATIVE STUDY USING ALUMINIUM PILLARED CLAYS AND ACTIVATED CARBON

J. E. Aguiar[1], B. T. C. Bezerra[1], A. C. A. Siqueira[1], D. Barrera[2], K. Sapag[2], D. C. S. Azevedo[1], S. M. P. Lucena[1], I. J. Silva Jr.[1,]

[1]Universidade Federal do Ceará, Centro de Tecnologia, Departamento de Engenharia Química, Grupo de Pesquisa em Separações por Adsorção – GPSA. Campus do Pici, Bloco 709, CEP. 60455-760, Fortaleza – CE, Brasil. Tel.: +55 (85) 3366-9611 (ext. 28); Fax: +55 (85) 3366 9601, [2]Universidad Nacional de San Luis, Laboratorio de Sólidos Porosos, INFAP-CONICET, San Luis, Argentina

Address correspondence to: I. J. Silva Jr , Universidade Federal do Ceará, Centro de Tecnologia, Departamento de Engenharia Química, Grupo de Pesquisa em Separações por Adsorção – GPSA. Campus do Pici, Bloco 709, CEP. 60455-760, Fortaleza – CE, Brasil. Tel.: +55 (85) 3366-9611 (ext. 28); Fax: +55 (85) 3366 9601 Email id: ivanildo@gpsa.ufc.br

Abstract

The aim of this work was evaluate the adsorption properties of anionic dye Reactive Black 5 (RB5) and cationic dye Methylene Blue (MB) from salted aqueous solution using natural clay, aluminum pillared clay (Al-PILC) and activated carbon. The textural properties of the materials were obtained by N_2 adsorption at 77 K and structural properties of natural and pillared clays were determined by X-ray diffraction. The effect of pH, contact time, initial concentration of dye and influence of the addition of NaCl were evaluated by batch adsorption. Adsorption isotherms of Al-PILC, in different salt concentration, were compared with natural clay and activated carbon. The adsorption isotherms were well fitted by Langmuir and Langmuir-Freundlich models. The process of pillaring only improved the adsorption of the anionic dye RB5. Depending on the system adsorbent/adsorbate analyzed, the salt concentration can either help or hinder dye adsorption. We found that a special morphology formed during the process of pillaring greatly increased adsorption of the MB cationic dye in the range of high salt concentrations. This unexpected result may help in developing new pillarization strategies to treat effluents with high salt content.

KEYWORDS: pillared clay, activate carbon, adsorption, dye removal.

ACCEPTED MANUSCRIPT

1. INTRODUCTION

The contamination of rivers and lakes with dyes causes visual pollution and serious damage to wild fauna and flora (1). Discharging dyes into the hydrosphere can cause environmental damage as the dyes give water an undesirable color (2) and reduce sunlight penetration, with some dyes also being toxic/carcinogenic (3). A considerable amount of research on wastewater treatment has focused on the elimination of reactive dyes, essentially for three reasons: firstly, reactive dyes represent 20–30% of the total dye market (4); secondly, large fractions of reactive dyes (10–50%) are wasted during the dying process (up to 0.6–0.8 g dye/dm3 can be detected in dyestuff effluent); thirdly, in the textile processing industry many processing steps are carried out discontinuously, resulting in different process streams from the same processing steps. More than 80% of the salt and 90% of the colour is discharged with the dyebath and first rinsing bath. Every day about 600-700 t of hosiery fabrics are processed requiring 400-500 tons of salt. The salt used is either sodium chloride (NaCl) or sodium sulphate (Na_2SO_4). This generates large quantity of effluent, and the total dissolved solids (TDS) in the treated effluent are in the range of 5000-7000 mg/l with chloride in the range of 2000-3500 mg/l as compared to the tolerance limits. The high level of TDS and chlorides is due to the salt addition in the dyeing process for the fixation of dyes into the fabric (5). Furthermore conventional wastewater treatment methods, which rely on aerobic biodegradation, were found to be inefficient for complete elimination of many reactive dyes (2) and it is difficult to remove reactive dyes using chemical coagulation due to the dyes' high solubility in water (6-8).

Adsorption has been studied as an alternative to conventional processes, because it usually demands small areas of installation and provides high throughputs. According with these aspects, there are several works with low-cost materials to be used as adsorbents for dye removal (9).

Among the different adsorbents, the natural clays type smectites have been used extensively, but they present some difficulty due to their thixotropic and hydrophilic properties. A modified material from clays, denominated pillared clays, has received attention due to the development of higher surface area and porosity as compared to natural clays. These materials have a higher acidity and lower hydrophilicity than the former natural clays, furthermore it is an abundant natural raw material compared to an adsorbent traditionally used for wastewater treatment, activated carbon. In general, pillared clay improves the efficiency in processes of adsorption and catalysis, and they are also widely used in the removal of different compounds (10), but studies about pillared clay dye removal are still scarce.

The main focus of this work will be evaluate the dye removal using aluminum pillared clay for anionic (Reactive Black 5) and cationic (Methylene Blue) dyes in the low (up to 0.2 mol/L) and high (1.0 mol/L) concentration range of NaCl. Initial pH, contact time and initial dye concentration influence were investigated by batch system. Because the charged surface of clay is strongly influenced by NaCl, we also investigate the adsorption behavior of the dyes onto activated carbon material which is neutral. This will help isolate the NaCl influence in the adsorbent and adsorbates since the literature data are discrepant. The study showed a rather complex picture to the influence of NaCl on dye adsorption capacity for anionic and cationic dyes on charged and neutral adsorbents.

2. MATERIAL AND METHODS

In this study aluminum pillared clay (Al-PILC) was synthesized from a natural clay montimorillonite from the Cuyo region - Province of San Juan - Argentina.

Norit GAC 1240 PLUS activated carbon was gently provided by Norit Inc. (Netherlands). According to the specifications furnished by the supplier, this carbon is an acid washed granular activated carbon which offers good adsorption properties for the removal of impurities from chemical, food, pharmaceutical and water applications. This material has been reported as neutral pH.

2.1. Aluminum Pillared Clay Synthesis

The pillaring clay process was carried out following the method reported by Roca Jalil et al. (11)**.** The pillaring agent (oligocation) was obtained by the hydrolysis of a 0.2 M solution of $AlCl_3.6H_2O$ with a solution of 0.5 M NaOH with an $OH^-/Al3^+$ ratio of 2. The NaOH solution was slowly added at 60 °C under stirring for 12 hours. The addition of the oligocation was dropwise incorporated into a 5 % suspension of natural clay. The suspension was maintained under stirring for 12 hours. The solids were then washed in dialysis membranes immersed in distilled water up to reach a conductivity value smaller than 10μS/cm, dried at at 60 °C for 12 hours and calcined at 500 °C for 1 hour at a heating rate of 10 °C / min.

2.2. Dyes

Reactive Black 5 (RB5) and Methylene Blue (MB) were purchased from Sigma (EUA). RB5 is a anionic sulfonated diazo reactive dye type and has the molecular formula $Na_4O_{19}S_6C_{26}H_{21}N_5$ with a molar mass of 991.83 $g \cdot mol^{-1}$. It is an organic dye, water-soluble, detectable at UV-visible range at a wavelength of 601.5 nm. Figure 1 shows the molecular structure of RB5. Methylene blue (methylthioninium chloride) molecular structure is shown in Figure 2. It is an aromatic chemical compound that is often used as an indicator in chemical reactions. It is an organic dye, poorly water soluble, UV-detection at 650 nm in the visible range. Its molecular formula is $C_{16}H_{18}N_3SCl$, molar mass of 319.85 $g \cdot mol^{-1}$.

For each dye a calibration curve at the maximum wavelengths absorbance was obtained from a scanning procedure using a UV/Vis spectrophotometer (Thermo Scientific Biomate 3, USA).

2.3. Elemental Composition, Structural And Textural Characterization

The chemical analysis of natural clay was performed by Inductively Coupled Plasma (ICP-OES). The sample was disintegrated according to ISO 11466 and its amount was calculated as the oxide. The Si which was determined by gravimetry and Na and K by flame photometry. From these results we investigated the cation exchange capacity (CEC) and the structural formula of natural clay. From these data and considering the percentage of the other minerals present in the raw material, the structural formula of the montmorillonite (sample fraction lower than 2 μm) was obtained following the method used by Roca Jalil et al. (11).

X-ray fluorescence analyses were performed in order to quantify the amount of Al after pillaring process. The loss on calcination was obtained by calculating the percentage decrease of the mass of the material calculated from 1 g of the sample when the same is subjected to calcination at 800 °C for 1 h with a heating interval of 10 °C/min.

Structural properties of the natural and pillared clay were analyzed by X-ray diffraction (XRD), in a RIGAKU diffractometer using Ni-filtered Cu Kα radiation over the 2θ range from 2 to 70 ° at scan speed of 1 °/min.

The textural characterization of the natural and pillared clay was performed by N_2 adsorption-desorption isotherms at 77 K (Micromeritics, ASAP 2000). The samples were previously degassed at 200 °C for 12 h. The specific surface area (S_{BET}) was estimated by the BET method (12) in the relative pressure range between 0.012 and 0.100 for natural clay and range between 0.0025 and 0.075 for Al-PILC. The total pore volume (V_{TP}) was obtained using Gurvich rule from the adsorption branch at a relative pressure of 0.98. Micropore volume ($V_{\mu P}$) of both natural and pillared clay was calulated with the t-plot method by using the t-equation of de Boer de Boer et al. (13). Taking into account the p/p^0 applicability range of this method is between 0.1 and 0.75 (14), the exact linear region was found in the following p/p^0 ranges for the materials under study were 0.202 – 0.301 for natural clay and 0.35 – 0.50 for Al-PILC. The volume of mesopores was calculated as the difference between (V_{TP}) and ($V_{\mu P}$). The pore size distributions were obtained by the NLDFT method. The NLDFT not was the best method to analyze the PSD of this kind of material and estimating the pore size. The micropore size distribution (MPSD) was analyzed using the model proposed by Horvath Kawasoe (HK) by (14).

The textural properties of activated carbon were measured by N_2 adsorption/desorption experiments at 77 K using an automatic sorptometer Autosorb 1 C (Quantachome, USA). The specific surface area was calculated using the BET methodology and micropore volume was determined using the Dubinin–Radushkevich (DR) equation, according to the procedure described by (12). The total pore volume was obtained from the N_2 volume adsorbed at a relative pressure of 0.95. The mesopore volume was obtained by subtracting the micropore volume from the total pore volume. The pore size distributions were calculated by applying the density functional theory (DFT) to the N_2 isotherm data. Activated carbons were dried 2 h at 140 C in muffle furnace microprocessor brand Tecnal (model EDGCON 3P - Brazil) before use.

2.4. Adsorption In Stirred Tank

In order to obtain the adsorption data in batch system, 20 mL of dye solution was added to 50 mL conical tubes containing 0.015 g of natural clay, Al-PILC and activated carbon. Several batch experiments were carried out in order to obtain information about the effect solution pH, initial dye concentration, and contact time. After prepare dye stock solutions, adsorption experiments were performed in a rotatory shaker (Tecnal TE-165, Brazil). At the end of experiments the supernatant were collected and centrifuged for 10 min at 10000 rpm (refrigerated micro centrifuge Cientec CT – 15000R). For the pH investigation, initial pH (2.0, 4.0, 7.0, 9.0 and 12.0) solutions of dyes were adjusted with concentrated HCl and NaOH solutions and batch adsorption experiment was performed. After that, the kinetic adsorption experiments were performed. For this aim, the samples were collected from the experimental tubes at pre-determined time

intervals. Adsorption isotherms were determined by analyzing the residual dye concentration from aqueous solution at increasing initial concentrations. For this aim, solutions of different dye initial concentration (25 – 300 ppm) in the presence of NaCl (0.0, 0.1, 0.2 and 1.0 mol/L) were evaluated. Salt concentrations were estimated according to the optimal dosage used in textile processing and maximum dosage discharged in effluent.

Dye amount adsorbed in the solid phase (adsorption capacity – q) was calculated according to Equation (1):

$$q^* = \frac{V(c_0 - c_{eq})}{m_{ads}} \qquad (1)$$

here c_0 (mg/mL) and c_{eq} (mg/mL) are the initial and the final (equilibrium) concentration of dye in liquid phase, V (mL) is the volume of solution, and m_{ads} (g) is the dried-weight of adsorbent.

The concentration of each dye in the supernatant solutions, before and after the adsorption experiments, was determined in UV/Vis spectrophotometer (Thermo Scientific Biomate 3, USA). All the adsorption experiments were performed twice at controlled temperature (22ºC ±1ºC).

In order to describe the behavior of the adsorption isotherm, the equilibrium data were correlated with Langmuir (L) and Langmuir-Freundlich models, as follows:

$$q^* = \frac{q_{\max} k_L c_{eq}}{1 + k_L c_{eq}} \qquad (2)$$

$$q = \frac{q_{\max}\left(k_{LF}c_{eq}\right)^{b}}{1+\left(k_{LF}c_{eq}\right)^{b}} \qquad (3)$$

where q_{max} (mg/g) is the maximum adsorption capacity, k_L (mg/L) is the Langmuir equilibrium constant, k_{LF} (mg/L)$^{1/b}$ is the constant of Langmuir-Freundlich, b is the constant of heterogeneous Langmuir-Freundlich.

Dye removal percentage was calculated using following equation:

$$\text{Dye removal}\ (\%) = \frac{c_0 - c_{eq}}{c_0} x100 \qquad (4)$$

3. RESULTS AND DISCUSSION

3.1. Characterizations

3.1.1. Natural And Pillared Clay

Figure 3 shows the XRD diffractogram of the natural and pillared clays. The natural clay exhibits a peak at 12.6 Å, which is commonly assigned to the basal spacing 001 (d_{001}). In pillared clays, the peak d_{001} appears in a lower 2θ value, with a d_{001} of 18.6 Å, which is a specific indication about the enlargement of basal spacing of the clay (15). Figure 3 also shows that pillared process affects only the basal spacing (d_{001}) in the natural clay, but do not change the structure, although little differences in intensity are appreciated. Basal spacing value depends of nature and type of cations exchange and the hidratation state of them and it is common that d_{001} be

modified. However other picks showed in the Figure 3, suggest that the natural clay structure was not affected in the pillared materials.

N_2 adsorption-desorption isotherms at 77 K for the natural clay and Al-PILC are shown in Figure 4. N_2 isotherm for the natural clay shows a typical behavior of montmorillonite. It is an isotherm type II with hysteresis type H3, showing indicative of an association of particles of lamellar aggregates, according to the IUPAC classification (16)**.** The presence of hysteresis is connected to the process of filling and emptying pores by capillary condensation. It is a typical characteristic of mesoporous materials domain (17, 18). This type of hysteresis is typical of such materials having regular pores, with cylindrical or polyhedral shape and open ends, such as clays. According to the classification IUPAC, the adsorption isotherm corresponding to Al-PILC is a type IV isotherm. The inflection point of the isotherm corresponds to the formation of the first occurrence of the adsorbed layer covering the entire surface of the material. The amount adsorbed at low values of P/Po is related to the presence of micropores as consequence the pillaring process. The hysteresis is H4 type corresponding to mesopores between parallel plates.

In Table 1 are shown the textural properties of the Al-PILC in comparison with natural clay. The specific surface area, micropore and total pore volumes are increased about eight, ten and two times, respectively. While the mesopore volume kept the same value after the pillaring process. The generation of micropores is concerned to the incorporation of pillars between the layers of the natural clay.

Figure 5 shown the pore size distribution obtained by the Non Local Density Functional Theory (NLDFT) model, where can be observed the presence of a large number of micropores with a values about of 13 Å.

The mesopore size distribution obtained by the BJH method of adsorption branch showed that these pores are widely distributed throughout the range predominantly mesopores ranging from 20 to 500 Å. This result is not shown here, but it is mentioned because the presence of mesoporous in the adsorbent is necessary to conduct the adsorbent molecules to the micropores region.

Chemical analysis of natural clay were shown as follows: 1.24 wt% Fe_2O_3; 0.30 wt% K_2O; 0.90 wt% CaO; 1.37 wt% TiO_2; 0.01 wt% MnO; 59.37 wt% SiO_2; 14.84 wt% Al_2O_3; 3.13 wt% MgO; 0.06 wt% P_2O_5; 0.07 wt% ZrO_2; 2.14 wt% Na_2O; 15.00 wt% and PPC for a total compounds of 98.43 wt%. The CEC of the clay mineral obtained this way was 0.62 meq/g. According to the results, natural clay formula were obtained and expressed as

$(Al_{0.20}\ Si_{7.80})_{IV}\ (Al_{2.69}\ Fe_{0.15}\ Mg_{1.11}\ Mn_{0.02})_{VI}\ O_{20}\ (OH)_4\ M_{1.41}$. The coordination's IV and VI indicate the atoms numbers located at each position in the tetrahedral and octahedral clay.

3.1.2. Activated Carbon

Figure 6 showed the N_2 adsorption/desorption isotherm at 77 K onto activated carbon. It resembles a type I isotherm established by IUPAC and BBDT without the presence of hysteresis, which characterizes the presence of micropores in the material. The carbon isotherm shows that at low relative pressures for adsorbing a considerable volume of gas indicates the presence of micropores. The

textural properties of activated carbon obtained by BET analysis are presented in Table 1. This material showed a surface area of 688 m^2g^{-1}. The distribution of pore size according to the BJH method is shown in Figure 7 which shows that most of the activated carbon structure is constituted by micropores. A uniform pore distribution allows infer that this material exhibits large amount of pores in the range 1 to 10 nm.

3.2 Experiments In Stirred Tanks

3.2.1. Effect Of Initial Ph

pH solution is an important operational aspect that should be taken into account because it affects the surface charge of adsorbent and also the degree of ionization of materials in solution (19). So, the effect of pH for adsorption of RB5 and MB were studied in the pH range of 2 –12. Figures 8 and 9 show the dye removal percentage and amount adsorbed with natural and pillared clay to RB5 and MB. As can be seen, the maximum adsorbed amounts were reached at pH 2.0 to RB5 and pH 12.0 to MB. The adsorption capacity decreased when the initial pH increased from 2 to 12 for RB5 and when the initial pH decreased from 12 to 2 for MB.

It should be considered that RB5 and MB dyes belong to different classes and different kind of interactions can be found. As reported by (20), dye adsorption involves several attractive forces such as ionic interaction, van der Walls forces, hydrogen bonding and covalent. Depending on the dye chemical composition one or more forces act in the adsorption process. According to (21), in aqueous solution anionic dyes carry a net negative charge due to the presence of sulphonate (SO^{-3}) groups, while cationic dyes carry a net

positive charge due to the presence of protonated amine or sulfur containing groups**.** Pillared clay used in this study has negative charges in aqueous solution resulting from isomorphic substitution and aggregation of Al^{3+} cations in natural clay. The point of zero charge (pHpzc) for pillared clay also needs to be considered. The pHpzc for pillared clay has been reported as about 4.4 - 5.0 (11, 22-23). At pH values above the pHpzc of the adsorbent, the surface of adsorbent particles is negatively charged. As expected result, the adsorption and dye removal of MB cationic dye increase for pH above the pHpzc. The opposite occurs for RB5 anionic dye. At a pH above 2, a decrease in adsorption takes place for RB5 dye due to repulsion between anionic dye molecules and negatively charged adsorbent surface.

The pH effect on dye adsorption observed in this study may be explained by protonation of clay surfaces and electrostatic interaction between clay and dye molecules. The same phenomenon was observed by (5, 6). As mentioned before, Al-PILC used in this study has negative charges in aqueous solution. Thus, it is possible to also occur hydrogen bond interactions between (OH^-) groups of adsorbent and ($-SO^{3-}$), (C=N) and aromatic groups of the RB5 and MB dyes.

The pKa of MB is 0.04 hence, MB is completely ionized at pH greater than 0.04 and serves as a cationic species with charge positive (24). Reactive Black 5 has pKa values lower than zero due to their two sulfonate groups and another two sulfato-ethyl-sulfone groups, with negative charges even in highly acidic solutions (25). A significant electrostatic attraction exists between the positively and negatively charged cationic and anionic dye and the charges of adsorbents surface exists due to the ionization of functional groups.

It is seen that the most effective pH for the adsorption of RB5 and MB onto AL-PILC is 2 and 12, respectively. Therefore, further

experiments were conducted at these pH values. It can also be seen in Figure 8 and 9 that Al-PILC have higher adsorption capacities and removal percentage for RB5 and MB than natural clays.

Figures 10 and 11 shows the influence of the initial pH on the adsorption behavior of the dyes onto activated carbon. There was no significant influence of pH on dyes uptake. Therefore, the selected pH for the adsorption experiments the kinetic was set at pH 12, this being the optimal considering operational and environmental issues.

The fact that dye uptake is not a function of the solution pH may be due to a number of reasons. The zeta potential activated carbon surface is clearly influenced by the pH, being positive at pH values lower than 7.5 and negative at pH values higher than 7.5. Therefore, electrostatic interactions between reactive dyes and the adsorbent are not be the main driving forces within the process. Van der Waals forces are probably responsible for the adsorption process (i.e., physical adsorption), which is common in the adsorption of organic compounds from aqueous solutions onto carbonaceous materials. Galán et al., (26), ascertained the same behavior when the influence of pH on the adsorption of RB5 in a mesoporous activated carbon was negligible.

3.2.2. Kinetics And Adsorption Isotherms

The kinetic profiles of RB5 and MB on Al-PILC, natural clay and activated carbon are shown in Figures 12 and 13. It was possible to observe a rapid decrease of dye concentration in the initial instants of contact reaching the equilibrium between 40 and 60 minutes. Among this, it was also observed that kinetic profiles for both dyes in both materials only differ in terms of amount adsorbed at the

equilibrium; the time to reach the equilibrium was independent of initial concentrations for both RB5 and MB dyes**.**

The adsorption isotherms of RB5 and MB dyes on natural clay, Al-PILC and activated carbon are shown in Figures 14 and 15 as well as the influence of NaCl concentration on the adsorption. The experimental data were well correlated with the Langmuir and Langmuir-Freundlich isotherms models. The results are shown in Table 2. Based on a statistical analysis of χ^2 and R^2, although both models showed a good fit to experimental data for both dyes in all adsorbents, LF model was more suitable to represent adsorption data.

Al-PILC has a higher adsorption capacity than the natural clay only for RP5. We did not associate this solely with the higher specific surface area, because that area increases did not improve MB adsorption. Probably negative charges have decrease in the clay platelike surface after pillarization. From the Figures 14 and 15, it can also be seen that the salt in the low concentration range, increase the adsorption capacity for Al-PILC/RP5 and activated carbon/MB. At higher salt concentrations (up to 1.0 mol/L) RB5 adsorption increases for Al-PILC/MB and activated carbon/MB. A possible explanation to that adsorption behavior was given in the next section 3.3.

3.3 Adsorption Mechanisms

3.3.1 Methylene Blue

Analyzing the adsorption behavior of MB, we observed that the uptake increases at low and high salt concentration for both materials. For pillared clay, small salt concentration results in almost imperceptible MB uptake increase, however we found a surprising elevated dye uptake in the NaCl high concentration range. In pillared clay, adsorption occurs exclusively on the surface. The main evidence of absence of interlayer adsorption is that even with seven times more surface area, the pillared clay has a small dye uptake performance. The pillarization resulted in a considerable interlayer gap increase (from approximately 4 to 10 -11 Å), but the presence of aluminum complexes between the clay sheets prevent access of the dye. The increase in superficial area is measured at 77 K with N_2 probe-gas. N_2 molecule is small enough to measures the area between the pillars, but this area is not accessible to the MB molecules. The exceptional uptake at high salt concentration can be explained by the natural tendency of the MB to form dimmers, trimmers and superior macroagregates (27) and a special morphology of the pillared clay (28). Pinnavaia et al. (28) had proposed a pillared clay model with large volumes of mesoporosity (Figure 16) created after the drying of the flocculated polyoxoaluminium-clay system. Our pillared clay mesoporosity (41% - Table 1) seems to match the size of the aggregates of the MB molecules in the region of high salt concentration, resulting in the record amount of adsorbed MB.

For activated carbon, the adsorption has been improved at the low concentration range of the salt and a few more in the region of high salt concentration. The activated carbon used (Norit GAC 1240), is essentially a microporous carbon with only 16% of volume of

mesopores (Table 1). The increase of the amount adsorbed on the activated carbon is due to the formation of MB dimers in the region of low NaCl concentration and clusters of upper order in the region of high concentration of salt. For activated carbon, clustering in trimers is sufficient to fill your small volume of mesopores, therefore the material promptly saturates.

3.3.2 Reactive Black 5

The salt concentration impairs the RB5 adsorption for both carbon and pillared clay material. Being larger than the MB (1.43 × 0.61 × 0.4 nm) (29), the RP5 (2.9 x 0.85 nm) (30) molecule accesses with difficulty the pores of activated carbon. The introduction of salt, even in small quantities, blocks still more, the access to the pores. This explains the reason for the adsorption in the salt concentration range of 0.1 mol/L and 1.0 mol/L was nearly equal. We do not expect any effect of NaCl charges on the activated carbon because its surface is neutral. The surface charges of the pillared clay suffers influence of salt. In the low concentrations range, the NaCl neutralizes the negative charges on the surface of the pillared clay allowing the adsorption of anionic dyes (30). However, at high concentrations, Na^+ and Cl^- ions can screen the charged sites of the adsorbents and adsorbates leading to a suppression of the electrostatic interactions (31). This must be the reason for the drastic drop of adsorption for the pillared clay in the range of high salt concentration. If RB5 molecules join together forming dimers or macroagregates (27), the morphology and size of these aggregates seems totally incompatible with the mesopores formed during the drying of the pillared clay. These aggregates would also be too large for the pores of activated carbon.

4. CONCLUSION

In this study we evaluate the dye adsorption of Methylene Blue and Reactive Black 5 dyes using natural, aluminum pillared clays and activated carbon.

It is not expected that anionic dyes adsorb onto clays because their surface charges are negative. We found however that pillaring promotes increased adsorption of anionic dyes not only by increased surface area but probably also by a decrease of negative surface charges.

The salt impaired or increased dye adsorption depending on the system examined. Comparison done with activated carbon, allowed to dissect where the salt influenced more strongly, if in the adsorbent or in the adsorbate.

The most surprising result came from the adsorption of MB in pillared clay in the range of high concentrations of salts (1 mol/L). The adsorbed dye mass (350 mg/g) exceeds even the best result obtained with activated carbon (250 mg/g) into a dye solution with a concentration of approximately 50 mg/ L.

The exceptional value in MB obtained for the pillared clay in the range of high salt concentration is associated with a special morphology developed during the pillaring procedure which creates mesoporosities with sizes compatible with the MB agglomerates. We note that other organic molecules with similar MB characteristics and the same tendency to formation of agglomerates can benefit from the network of mesopores created during the synthesis of aluminum pillared clays. This is a specially promising line of research for industrial effluents with high levels of salt.

ACKNOWLEDGEMENTS

The authors would like to thank CNPq (Universal 2010 Process Nº 474436-2010-1) and CAPES (project CAPG) for the financial support. The authors also would like to thank Universidad Nacional de San Luis – Argentina – INFAP-CONICET. Special thanks to Prof. Dr. Giorgio Zgrablich – *In memory*.

REFERENCES

1. Robinson, T.; Mcmullan, G.; . Marchant, R.; Nigam, P. (2001) Remediation of dyes in textile effluent: a critical review on current treatment technologies with a proposed alternative. *Bioresour. Technol.*, 77, 247–255.

2. Al-Degs, Y.S.; El-Barghouthi, M.I.; Khraisheh, M.A.; Ahmad, M.N.; Allen, S.J. (2004) Effect of surface area, micropores, secondary micropores and mesopores volumes of activated carbons on reactive dyes adsorption from solution. *Sep. Purif. Technol*., 39, 97–111.

3. Wang, S.; Boyjoo, Y.; Choueib, A.; Zhu, H. (2005) Removal of dyes from solution using fly ash and red mud. *Water Res,*. 39, 129–138.

4. Orfao, J.; SIlva, A.; Pereira, J.; Barata, S.; Fonseca, I.; Faria, P. (2006) Adsorption of a reactive dye on chemically modified activated carbons: influence of pH. *J. Coll. Interface Sci*., 296, 480–489.

5. Vishnu, G.; Palanisamy, S.; Joseph, K. (2008) Assessment of fieldscale zero liquid discharge treatment systems for recovery of water and salt from textile effluents. *Jour. Cleaner Prod.*, 10, 1081-1089.

6. Errais, E.; Duplay, J.; Darragi, F.; M'rabet, I.; Aubert, A.; Huber, F.; Morvan, G. (2001) Efficient anionic dye adsorption on natural untreated clay: Kinetic study and thermodynamic parameters. *Desalination*, 275, 74–81.

7. Errais, E. Reactivity of Natural Clay: Study of Adsorption Anionic Dyes. PhD Thesis, Strasbourg University, France (2011).

8. Gurses, A.; Dogar, C.; Yalcin, M.; Acikyildiz, M.; Bayrak, R.; Karaca, S. (2006) The adsorption kinetics of the cationic dye, methylene blue, onto clay. *J. Hazard. Mater. B,* 131, 217–228.

9. Oliveira, L.C.A.; Gonçalves, M.; Oliveira, D.Q.L.; Guerreiro, M.C.; Guilherme, L.R.G.; Dallago, R.M. (2007) Solid waste from leather industry as adsorbent of organic dyes in aqueous-medium. *J. Hazard. Mater.*, 141, 344–347.

10. Sapag, K.; Girón, R.L.; Mendioroz, S. (2001) Proper stability in porous media based in a natural clay. *Granular Matter,* 3 1/2, 131-135.

11. Roca Jalil, M.E.; Vieira, R.S.; Azevedo, D.; Baschini, M.; Sapag, K. (2013) Improvement in the adsorption of thiabendazole by using aluminum pillared clays. *App. Clay Sci.*, 71, 55-63.

12. Rouquerol, J.; Llewellyn, P.; Rouquerol, F. (2007) Is the BET equation applicable to microporous adsorbents? *Stud. Surf. Sci. Catal.*, 160, 49-56.

13. de Boer, J.H.; Lippens, B.C.; Linsen, B.G.; Broekhoff, J.C.P.; van den Heuvel, A; Osinga, T.J. (1966) The t-curve of multimolecular N_2 adsorption, *J. Colloid Interface Sci.*, 21, 405-414.

ACCEPTED MANUSCRIPT

14. Gil, A.; Korili, S.A., Vicente, M.A. (2008) Recent advances in the control and characterization of the porous structure of pillared clay catalysts, Catal. Rev. Sci. Eng, 50, 153-221.

15. Valverde, J.L. (2005) Preparation and characterization of Fe-PILCS: Influence of the synthesis parameters. *Clays Clay Miner.*, 53, 613-621.

16. Sing, K.S.W.; Everett, D.H.; Haul, R.A.W.; Moscou, L.; Pierotti, R.A.; Rouquerol, J.; Siemieniewska, T. (1985) Reporting physisorption data for gas/solid systems with special reference to the determination of surface area and porosity. *Pure Appl. Chem.*, 57, 603-619.

17. Marsch, H.; Reinoso, F.R. *Activated Carbon*, Elsevier, (2006).

18. Auxilio, A.R.; Andrews, P.C.; Junk, P.C.; Spiccia, L. (2009) The adsorption behavior of C.I. Acid Blue 9 onto calcined Mg-Al layered double hydroxides. *Dyes and Pigm.*, 81, 103-112.

19. Karaoğlu, M.H.; Dogan, M.; Alkan, M. (2010) Removal of reactive blue 221 by kaolinite from aqueous solution. *Ind. Eng. Chem.*, 49, 1534-1540.

20. Guaratini, C.C.I.; Zanoni, M.V.B. (2000) Corantes têxteis. *Quím. Nov*., 23, 71-78.

21. Netpradit, S.; Thiravetyan, P.; Towprayoon, S. (2004) Adsorption of three azo reactive dyes by metal hydroxide sludge: effect of temperature, pH, and electrolytes. *J. Coll. Interface Sci.*, 270, 255–261.

22. Avena, M.J. (2006) Acid–Base Behavior of Clay Surfaces in Aqueous Media. *Encyclopedia Surf. Coll. Sci.*, 17 – 46.

23. Manohar, D.M.; Noelite, B.F.; Anirudhan, T.S. (2005) Removal of vanadium (IV) from aqueous solutions by adsorption process with aluminum-pillared bentonite. *Ind. Eng. Chem. Res.*, 44, 6676 – 6684.

24. Weng, C.H.; Lin, Y.T.; Tzeng, T.W. (2009) Removal of methylene blue from aqueous solution by adsorption onto pineapple leaf powder. *J. Hazard. Mater*., 170, 417-424.

25. Cardoso, N.F.; Pinto, R.B.; Lima, E.C.; Calvete, T.; Amavisca, C.V.; Royer, B.; Cunha, M.L.; Fernandes, T.H.M.; Pinto, I.S. (2011) Removal of remazol black B textile dye from aqueous solution by adsorption. Desalination, 269, 92-103.

26. Galán, J.; Rodríguez, A.; Gomez, J.M.; Allen, S.J.; Walker, G.M. (2013) Reactive dye adsorption onto a novel mesoporous carbon. *Chem. Eng. J.*, 219, 62-68.

27. Hamlin, J. D.; Phillips, D. A. S.; Whiting, A. (1999) UV/Visible spectroscopic studies of the effects of common salt and urea upon reactive dye solutions. *Dyes and Pigm.*, 41, 137-142.

28. Pinnavaia, T. J.; Tzou, M.S.; Landau, S.D.; Raythatha, R.H. (1984) On the pillaring and delamination of smectite clay catalysts by polyoxo cations of aluminum. *J. of Molecular Catal*., 27, 195-212.

29. Pelekani, C.; Snoeyink, V.L. (2000) Competitive adsorption between atrazine and methylene blue on activated carbon: the importance of pore size distribution. *Carbon*, 38, 1423–1436.

30. Ip Alvin, W.M.; Barford, J.P.; Mckay, G. (2010) A comparative study on the kinetics and mechanisms of removal of Reactive Black 5 by adsorption onto activated carbons and bone char. *Chem. Eng. J.*, 157, 434–442.

31. Hu, Y.; Guo, T.; Ye, X.; Li, Q.; Guo, M.; Liu, H.; Wu, Z. (2013) Dye adsorption by resins: Effect of ionic strength on hydrophobic and electrostatic interactions. *Chem. Eng. J.*, 228, 392-397.

ACCEPTED MANUSCRIPT

Table 1 - Textural properties of the natural clay; Al-PILC and activated carbon.

Samples	**S_{BET} (m^2/g)**	**$V_{\mu P}$ (cm^3/g)**	**D_P (nm)**	**V_{TP} (cm^3/g)**
Natural Clay	43	0.01	3.7	0.08
Al-PILC	304	0.10	1.3	0.17
Activated Carbon	688	0.36	1.7	0.43

Table 2 - Langmuir and Langmuir-Freundlich isotherm parameters for RB5 and MB on natural clay; Al-PILC and activated carbon.

		Langmuir Model				**Langmuir-Freundlich Model**				
	Dyes	q_{max} **(mg/g)**	k_L **(mg/L)**	R^2	χ^2	q_{max} **(mg/g)**	k_L **$(mg/L)^{1/b}$**	b	R^2	χ^2
Natural	RB5	12.0(±0.38)	57.097(±5.957)	0.993	0.087	12.24(±0.98)	0.02(±0.003)	0.99(±0.15)	0.995	0.075
Clay	MB	25.4(±0.38)	17.49(±1.448)	0.996	0.282	26.69(±1.24)	11.3(±3.48)	0.83(±0.21)	0.997	0.243
Al-PILC	RB5	40.8(±1.07)	0.0207(±0.002)	0.995	0.766	37.44(±1.40)	0.02(±0.002)	1.22(±0.11)	0.997	0.509
	MB	49.4(±1.84)	0.0476(±0.009)	0.980	5.552	72.23(±11.1)	8.87(±0.84)	0.51(±0.08)	0.997	0.887
0.1 NaCl	RB5	43.0(±0.98)	0.0218(±0.001)	0.996	0.659	39.62(±1.32)	0.02(±0.002)	1.22(±0.10)	0.998	0.412
(mol/L)	MB	53.3(±2.09)	0.0468(±0.009)	0.978	7.117	82.69(±18.3)	8.96(±1.04)	0.48(±0.10)	0.996	1.46
0.2 NaCl	RB5	47.7(±0.76)	0.0241(±0.001)	0.997	0.514	46.17(±1.93)	0.03(±0.003)	1.07(±0.10)	0.998	0.554
(mol/L)	MB	64.0(±2.82)	0.0460(±0.010)	0.972	12.76	146.5(±54.5)	11.2(±3.19)	0.38(±0.066)	0.998	0.98
1.0 NaCl	RB5	6.15(±0.22)	0.025(±0.219)	0.988	0.045	5.50(±0.15)	0.03(±0.002)	1.51(±0.16)	0.995	0.02
(mol/L)	MB	474.9(±13.1)	16.77(±1.046)	0.998	32.38	465.8(±31.6)	17.0(±1.42)	1.02(±0.07)	0.998	37.2
Activated	RB5	147.3(±3.31)	0.070(±0.007)	0.993	18.26	163.2(±7.02)	0.05(±0.008)	0.76(±0.06)	0.998	6.51

Carbon	MB	187.4(±13.8)	2.317(±0.918)	0.895	662.5	256.6(±82.7)	0.38(±0.82)	0.38(±0.16)	0.958	312.6
0.1 NaCl	RB5	77.26(±3.16)	0.045(±0.008)	0.980	13.32	104.2(±16.4)	0.02(±0.01)	0.58(±0.10)	0.995	3.988
(mol/L)	MB	234.2(±19.4)	1.460(±0.560)	0.876	1171.6	375.3(±298.3)	0.10(±0.52)	0.33(±0.23)	0.929	781.7
1.0 NaCl	RB5	73.76(±4.62)	0.056(±0.02)	0.945	32.07	132.4(±85.1)	0.006(±0.02)	0.41(±0.18)	0.981	14.35
(mol/L)	MB	258.7(±13.8)	2.618(±0.88)	0.942	793.9	340.4(±66.3)	0.406(±0.52)	0.42(±0.12)	0.975	399.0

Figure 1 – Molecular structure of the dye Reactive Black 5 (RB5).

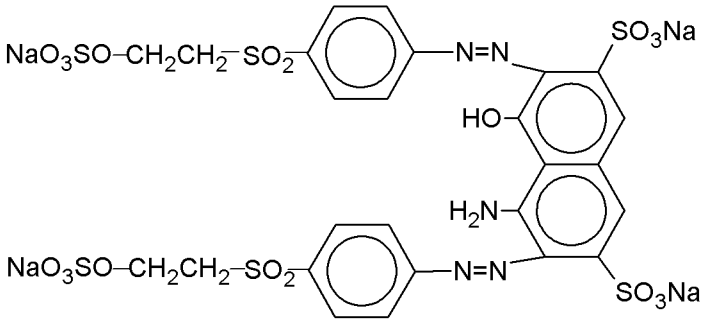

Figure 2 – Molecular structure of the dye Methylene Blue (MB).

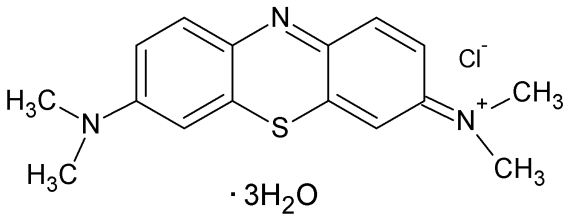

Figure 3 – Diffraction patterns obtained for the natural clay and Al-PILC: (M) Montmorillonite; (B) Boehmite; (C) Quartz; (F) Feldspar.

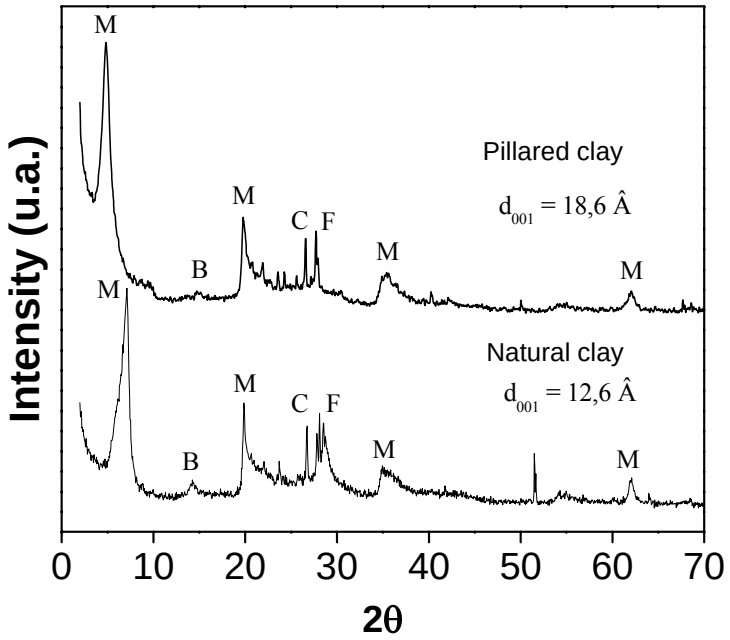

Figure 4 – Adsorption-desorption isotherms of N_2 at 77 K: (□) natural clay; (O) Al-PILC.

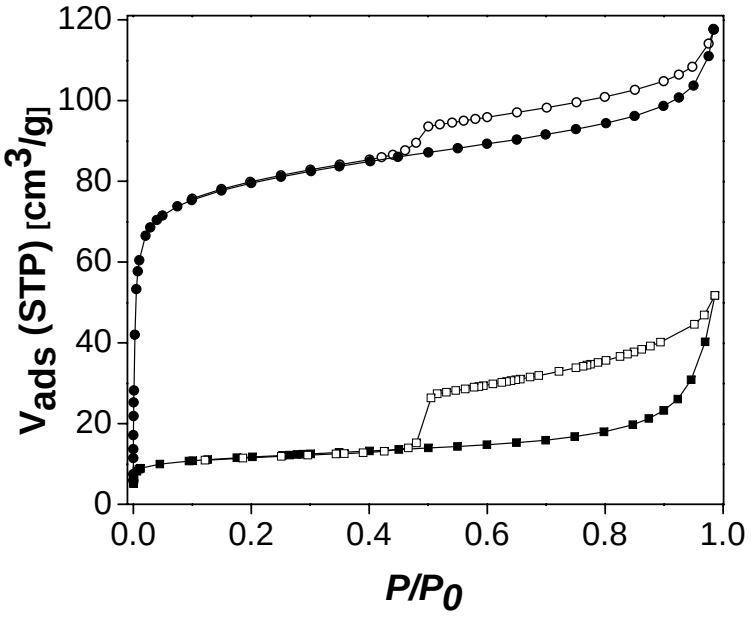

Figure 5 – Pore size distribution of pillared clay.

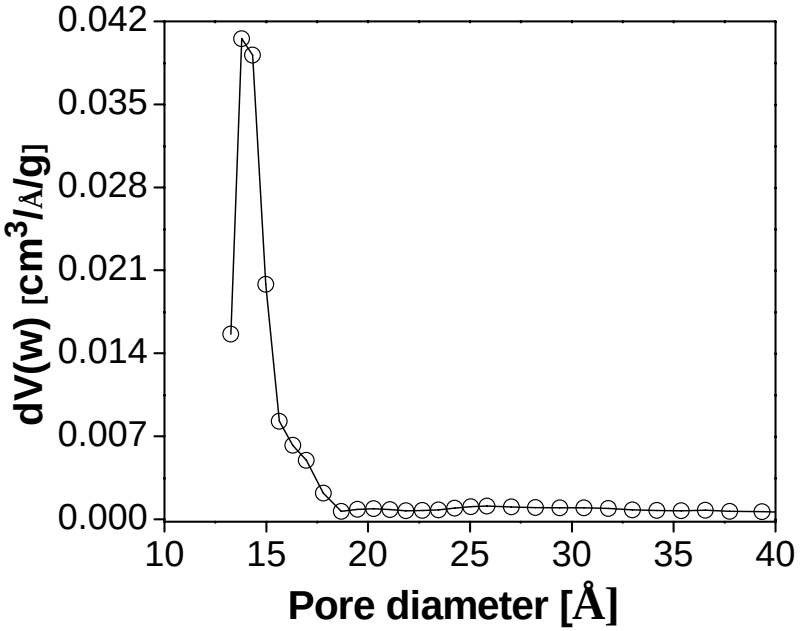

Figure 6 – Adsorption-desorption isotherms of at N_2 at 77 K activated carbon.

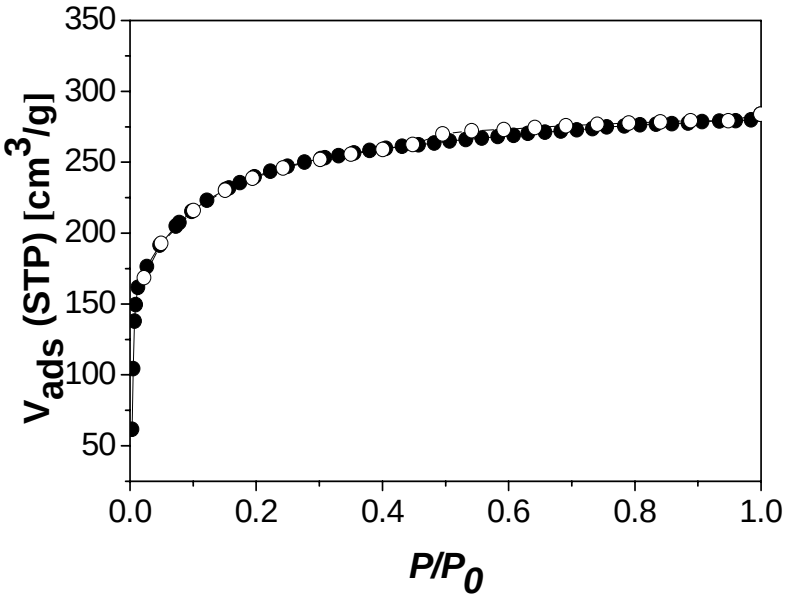

Figure 7 – Pore size distribution of activated carbon.

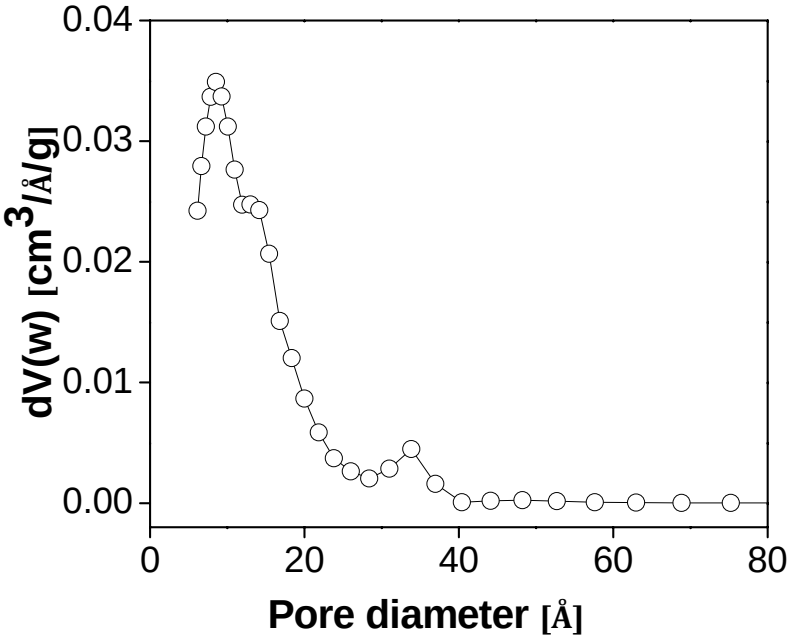

Figure 8 – Initial pH effect on RB5 adsorption on pillared clay and clay natural: ◊ amount adsorbed in natural clay; ◊ removal percentage in natural clay; □ amount adsorbed in Al-PILC; Δ removal percentage in Al-PILC.

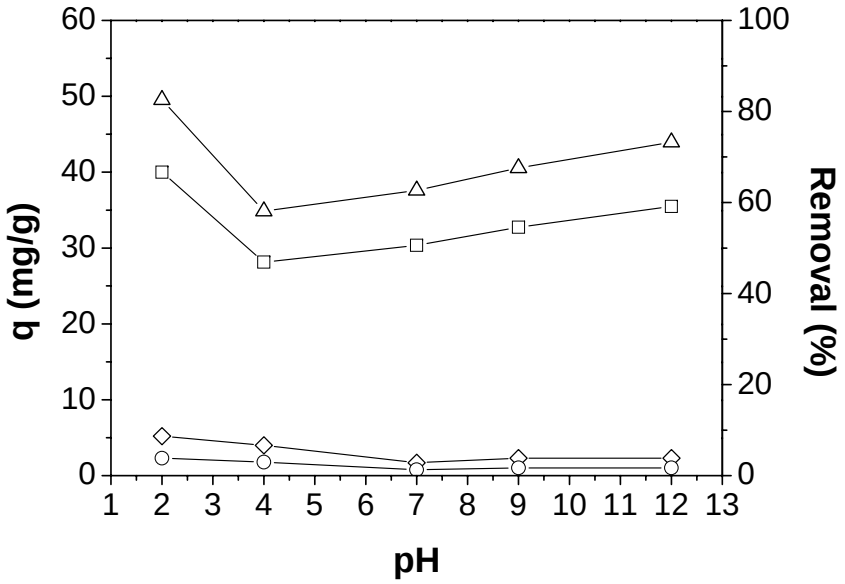

Figure 9 – Initial pH effect on MB adsorption on pillared clay and clay natural. : ◊ amount adsorbed in natural clay; ◊ removal percentage in natural clay; □ amount adsorbed in Al-PILC; Δ removal percentage in Al-PILC.

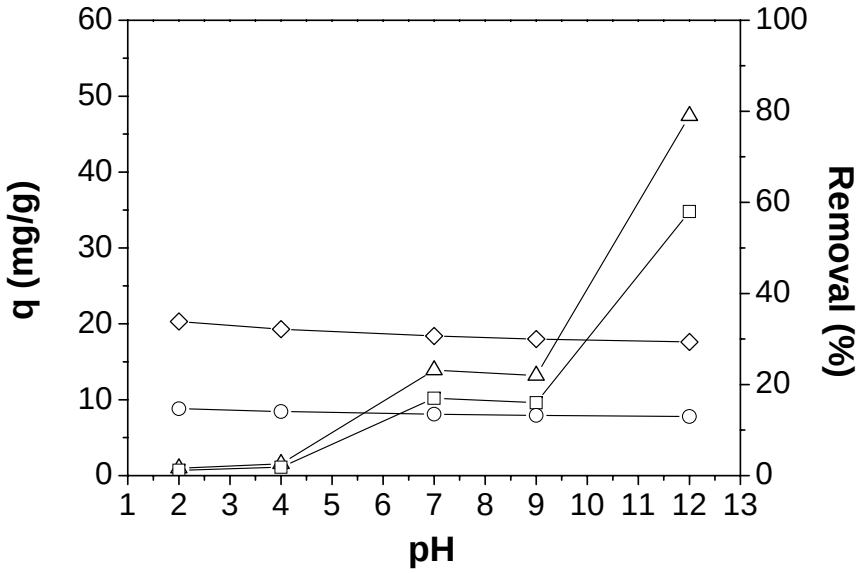

Figure 10 – Initial pH effect on RB5 adsorption on activated carbon: (□) amount adsorbed; (O) removal percentage.

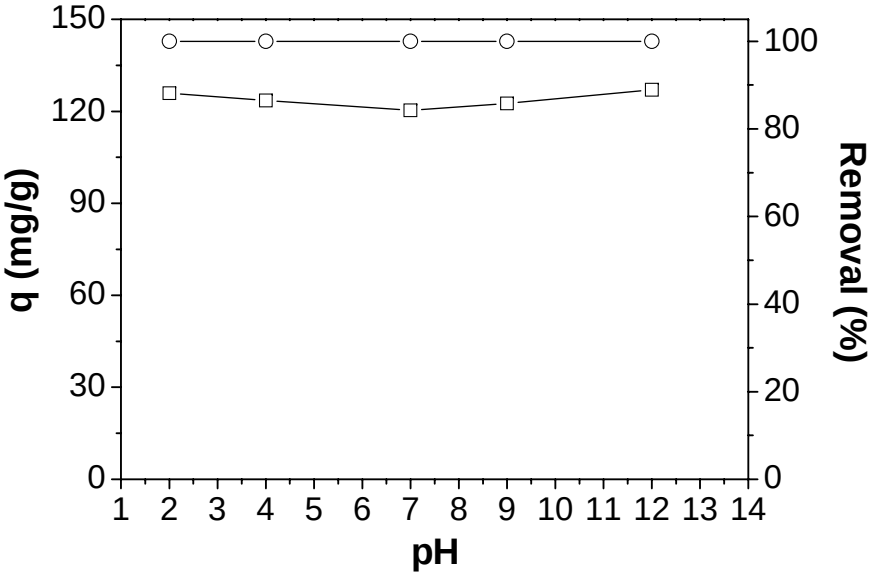

Figure 11 – Initial pH effect on MB adsorption on activated carbon: (□) amount adsorbed; (O) removal percentage.

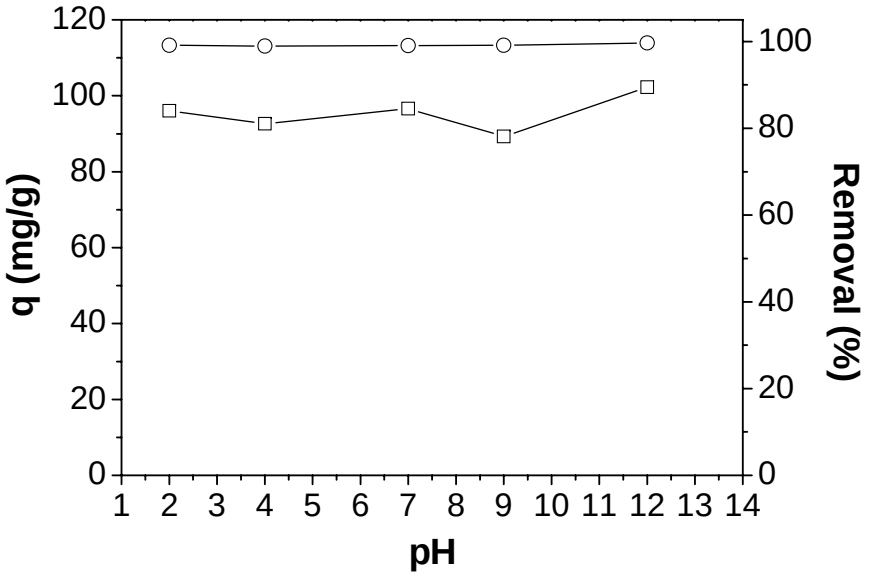

Figure 12 – Adsorption kinetics of RB5 in natural clay, Al-PILC and activated carbon: (□) 100 ppm of RB5 in Al-PILC; (O) 150 ppm of RB5 in AL-PILC; (Δ) 100 ppm of RB5 in natural clay and (◊) 100 ppm of RB5 in activated carbon.

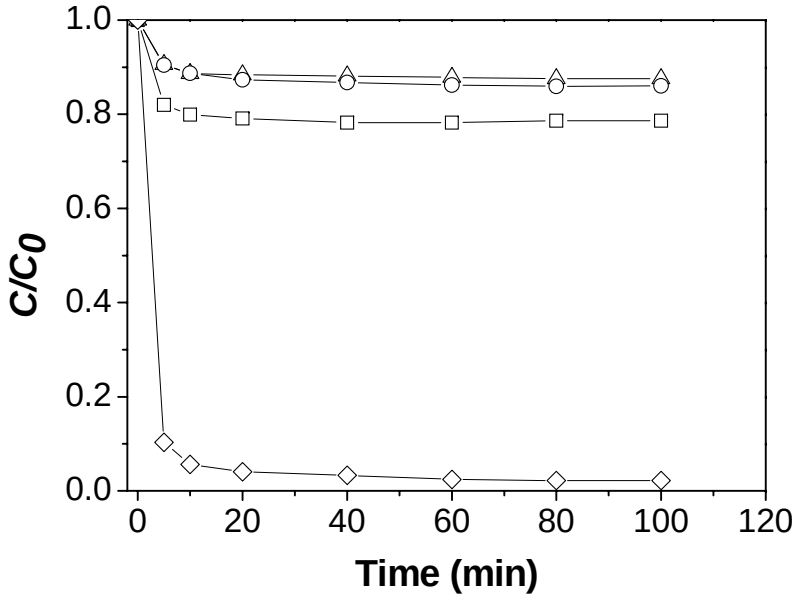

Figure 13 – Adsorption kinetics of MB in natural clay, Al-PILC and activated carbon: (□) 100 ppm of MB in Al-PILC; (O) 150 ppm of MB in Al-PILC; (Δ) 100 ppm of MB in natural clay and (◊) 100 ppm of MB in activated carbon.

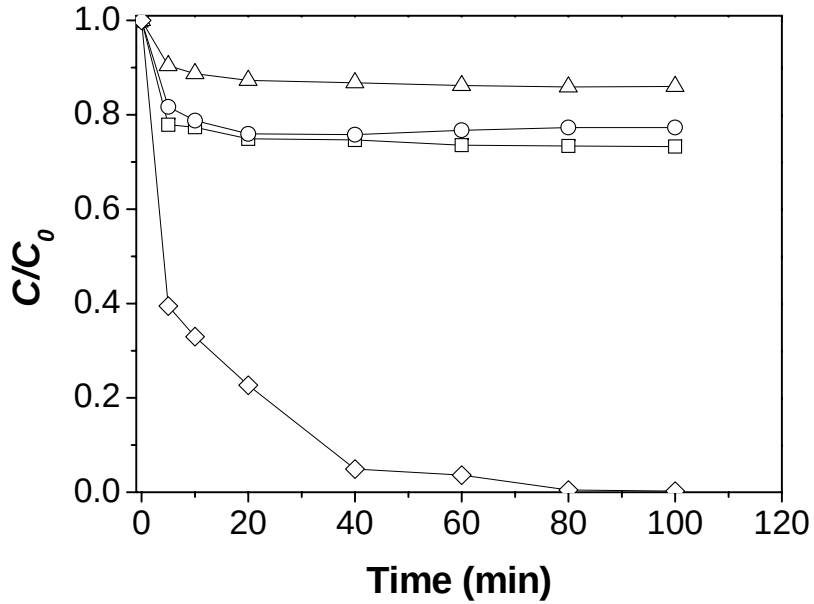

Figure 14 – Adsorption isotherm of RB5 in natural clay, AL-PILC and activated carbon: [a] natural clay and AL-PILC: (◊) natural clay; (□) 0.0 mol/L NaCl; (Δ) 0.1 mol/L NaCl; (O) 0.2 M mol/L NaCl and (∇)1.0 mol/L NaCl; [b] activated carbon: (■) 0.0 mol/L NaCl; (▲) 0.1 mol/L NaCl and (▼)1.0 mol/L NaCl.

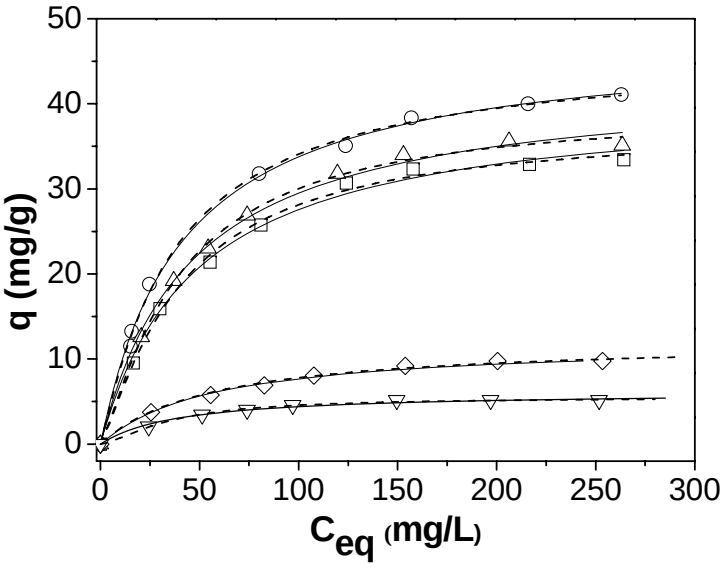

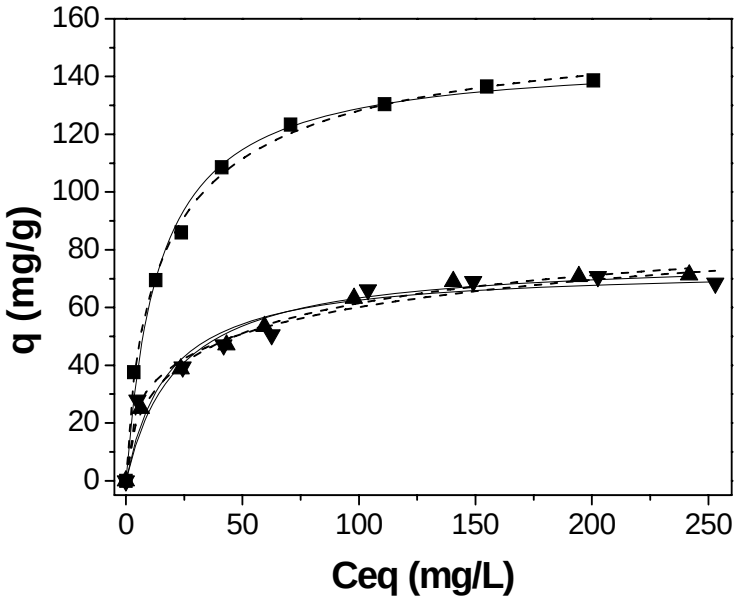

ACCEPTED MANUSCRIPT

Figure 15 – Adsorption isotherm of MB in natural clay, AL-PILC and activated carbon: [a] natural clay and AL-PILC: (◊) natural clay; (□) 0.0 mol/L NaCl; (Δ) 0.1 mol/L NaCl; (O) 0.2 M mol/L NaCl and (∇) 1.0 mol/L NaCl; [b] activated carbon: (■) 0.0 mol/L NaCl; (▲) 0.1 mol/L NaCl and (▼)1.0 mol/L NaCl.

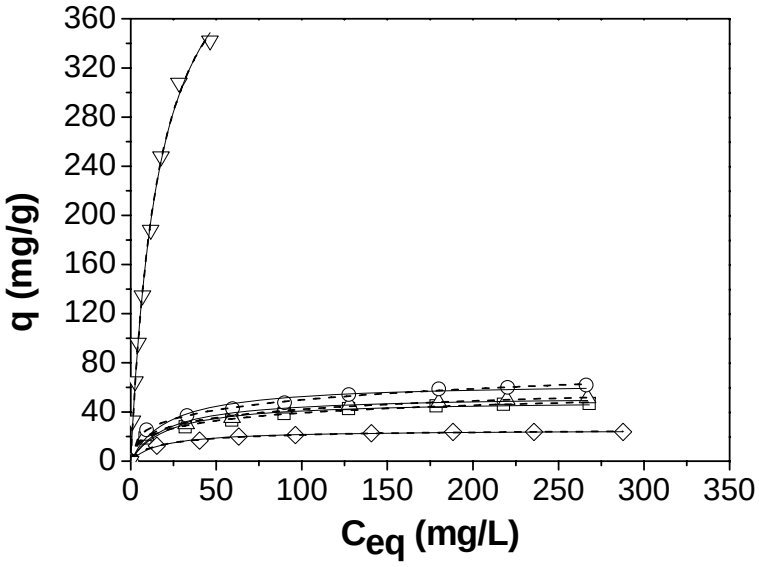

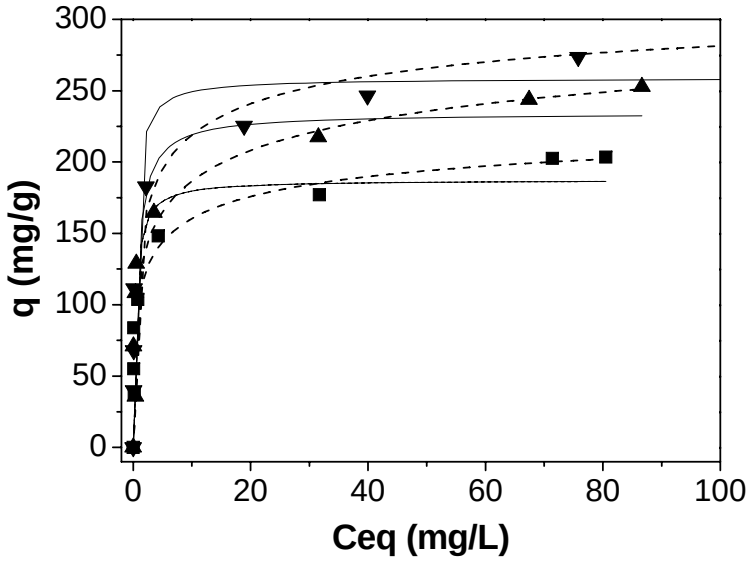

ACCEPTED MANUSCRIPT

Figure 16 – Morphology of pillared clay proposed by Pinnavaia (28). Red - clay sheet, Open circles - pillar and light blue - mesoporosities.